RSC Advances

PAPER

View Article Online
View Journal | View Issue

Cite this: *RSC Adv.*, 2020, **10**, 4218

PLGA nanoparticle preparations by emulsification and nanoprecipitation techniques: effects of formulation parameters

Karol Yesenia Hernández-Giottonini,[a] Rosalva Josefina Rodríguez-Córdova,[a] Cindy Alejandra Gutiérrez-Valenzuela,[b] Omar Peñuñuri-Miranda,[b] Paul Zavala-Rivera,[b] Patricia Guerrero-Germán[b] and Armando Lucero-Acuña*[b]

This study presents the influence of the primary formulation parameters on the formation of poly-DL-lactic-*co*-glycolic nanoparticles by the emulsification-solvent evaporation, and the nanoprecipitation techniques. In the emulsification-solvent evaporation technique, the polymer and tensoactive concentrations, the organic solvent fraction, and the sonication amplitude effects were analyzed. Similarly, in the nanoprecipitation technique the polymer and tensoactive concentrations, the organic solvent fraction and the injection speed were varied. Additionally, the agitation speed during solvent evaporation, the centrifugation speeds and the use of cryoprotectants in the freeze-drying process were analyzed. Nanoparticles were characterized by dynamic light scattering, laser Doppler electrophoresis, and scanning electron microscopy, and the results were evaluated by statistical analysis. Nanoparticle physicochemical characteristics can be adjusted by varying the formulation parameters to obtain specific sizes and stable nanoparticles. Also, by adjusting these parameters, the nanoparticle preparation processes have the potential to be tuned to yield nanoparticles with specific characteristics while maintaining reproducible results.

Received 24th December 2019
Accepted 13th January 2020

DOI: 10.1039/c9ra10857b

rsc.li/rsc-advances

Introduction

Polymeric nanoparticle (PNP) preparation techniques are of great interest in biomedical research, in particular for drug delivery applications. The objective of PNPs in drug delivery applications is to achieve drug release in a controlled manner; to be biocompatible with tissues and cells; to reach higher intracellular uptake than free drugs; to improve the stability of active substances; and to be able to target specific tissues.[1–3] An essential factor in the design of these systems is the size; the PNPs should be big enough to prevent fast incorporation into blood vessels but small enough to prevent elimination from the immune system.[4] The PNP preparation techniques should be analyzed and adapted to each active substance to meet all these characteristics. Besides, it is essential to study the PNP preparation techniques to allow the production of reproducible large batches.[5] The necessity to scale-up the PNP preparation process to the industrialized scale has been stated in earlier studies.[6,7]

Among the polymers used in the preparation of PNP, the most widely used is poly-DL-lactic-*co*-glycolic acid (PLGA). PLGA is successfully used in the research of drug delivery systems, because of its biodegradability and low systemic toxicity, it has also been approved by the US Food and Drug Administration (FDA) for medical applications.[8–11] PLGA can be formulated as PNP using several different methods, such as emulsification-evaporation, nanoprecipitation or solvent displacement, solvent diffusion, and phase-inversion; with sizes ranging from 10 to 1000 nm.[12,13] When encapsulating hydrophobic compounds, two of the most commonly used techniques are the emulsification-solvent evaporation technique and the nanoprecipitation technique.[14–16] The emulsification technique is based in a mixture of a volatile non-water miscible solvent and an aqueous solution, which are emulsified by the application of high shear force. Then the volatile solvent is evaporated, forming in the process the PNP. This method is advantageous because it is nontoxic, rapid in reaction rate, and produces very small particles.[17] Nevertheless, a disadvantage in the technique is the standardization for each specific drug, the high energy used in the process, which could affect the stability of certain drugs.[18,19] On the other hand, in the nanoprecipitation method, the nanoparticles are formed in one step.[20,21] Nanoprecipitation, involves the use of miscible solvents and its advantages include simplicity, good reproducibility, and low energy input.[22,23] After the nanoparticle formulation with most techniques, some potentially toxic impurities such as organic solvents, surfactant excess, residual monomers, and large polymer aggregates must be eliminated. Some of the most common particle purification

[a]*Nanotechnology Graduate Program, Department of Physics, University of Sonora, Hermosillo, Mexico*

[b]*Department of Chemical and Metallurgical Engineering, University of Sonora, Hermosillo, Mexico. E-mail: armando.lucero@unison.mx; Tel: +52-662-259-2105*

methods for laboratory scale include dialysis, gel filtration, evaporation under reduced pressure, and ultracentrifugation.[24] Several works analyze the experimental parameters of different techniques for the encapsulation of specific drugs.[25–34] The effect of some formulation parameters on the size of PLGA nanoparticles encapsulating bovine serum albumin, prepared by double emulsion solvent evaporation method, indicate that PLGA and PVA concentrations have a direct effect on the particle size.[35] Halayqa and Domańska analyzed the effect of some parameters in the emulsion-evaporation technique to improve the efficiency of encapsulation and size in the preparation of PNP loaded with perphenazine and chlorpromazine hydrochloride.[36] The influence of different experimental parameters on the incorporation efficiency of paclitaxel in the PLGA nanoparticles prepared by the interfacial deposition method was reported in the literature.[37] Also, Derman *et al.*, improve the encapsulation efficiency of caffeic acid phenethyl ester, using the oil in water (o/w) single emulsion solvent evaporation method, reporting high and sustained drug release.[38] The same single emulsion technique was reported for PLGA nanoparticles preparations with simultaneously loaded vincristine sulfate and quercetin, by evaluating six independent parameters.[39] The effects of different formulation parameters on particle size, zeta potential, drug loading efficiency and drug release of PLGA nanoparticles loaded with ciprofloxacin HCL and prepared by w/o/w emulsification solvent evaporation method is also reported in the literature.[40] The effect of process and formulation parameters using nanoprecipitation on prednisolone loaded PLGA nanoparticles was studied.[41] Also, Muthu *et al.*, varied the concentration of PLGA and risperidone in the preparation of nanoparticles to improve the encapsulation efficiency.[42] Govender *et al.* evaluated some formulation parameters to enhance the incorporation of a water-soluble drug (procaine hydrochloride) into PLGA nanoparticles.[43] Madani *et al.* analyzed the effect of formulation parameters over the size of paclitaxel-loaded PLGA nanoparticles prepared by the emulsion and the precipitation methods.[44] Other works have been focused not only in parameter studies but also in scale-up processes. Galindo-Rodríguez *et al.* made a comparative scale-up of three manufacturing processes; salting-out, emulsification–diffusion, and nanoprecipitation.[45] Also, He *et al.* worked in the scalable fabrication of size-controlled chitosan nanoparticles for oral delivery of insulin.[46] A comparison of the techniques of emulsion diffusion, solvent displacement, and double emulsion to prepare doxorubicin-loaded nanoparticles has also been reported in the literature.[47] Sah *et al.* provided the fundamentals into emulsion solvent evaporation/extraction, salting-out, nanoprecipitation, membrane emulsification, microfluidic technology, and flow focusing.[48] Mora-Huertas *et al.* describes the effect of the oil used in the recipes and preparation methods of nanoprecipitation and emulsification over the behavior of nanocapsules.[49] Paliwal *et al.* made a review of the production methods of polymeric and lipid nanoparticles, their scale-up techniques, and commercialization challenges.[50] Despite all the efforts in the encapsulation techniques of several actives into PLGA nanoparticles, is still essential to adapt these processes for the encapsulation of other different compounds. Therefore, this work aims to offer insights into the variable behaviors in the PLGA nanoparticles preparation processes to facilitate the encapsulation of other actives and for tune the nanoparticle-desired characteristics. Several factors that intervene in the PNP preparation processes were analyzed. In the emulsification-solvent evaporation technique, the polymer and tensoactive concentrations, the organic solvent fraction, and the sonication amplitude effects were analyzed. Similarly, in the nanoprecipitation technique were varied the polymer and tensoactive concentrations, the organic solvent fraction, and the injection speed. Additionally, the agitation speed during the solvent evaporation, the centrifugation speeds, and the use of cryoprotectants in the lyophilization process were studied. Nanoparticles were characterized by dynamic light scattering (DLS), laser Doppler electrophoresis, and scanning electron microscopy (SEM).

Materials and methods

Materials

PLGA acid terminated (50/50 DL-lactide/glycolide copolymer) with a molecular weight of 17 kg mol^{-1} (P17A), and PLGA (50/50 DL-lactide/glycolide copolymer) with a molecular weight of 153 kg mol^{-1} (P153) were received as gift sample from Corbion Purac, Gorinchem, The Netherlands. Polyvinyl alcohol (86–89% hydrolysis, low molecular weight, PVA) was obtained from Alfa Aesar, Ward Hill, Massachusetts, USA. Dichloromethane (DCM) was obtained from Fisher Scientific Inc., Fair Lawn, New Jersey, USA. Acetonitrile (AC) was obtained from Sigma Aldrich, Inc., St. Louis, MO, USA.

Preparation of PNP

PLGA nanoparticles were prepared by the single emulsification and the nanoprecipitation techniques.[14,23,51] Fig. 1 illustrates the PNP preparation scheme for both techniques and the parameters evaluated within the study. Also, Table 1 presents the values of the parameters considered in each experiment; these parameters were analyzed individually while the rest of the conditions and procedures were maintained constant, as a control. The control conditions and procedure in the single emulsification technique are the following: an organic solution (DCM) containing 10 mg mL^{-1} of PLGA was added into an aqueous solution of 5% of PVA (with an organic solvent fraction of 0.167). The mixture was then emulsified for 1 min at 75% amplitude (90 μm) under an ice bath using a QSonica 500 sonicator (QSonica LLC, Newtown, Connecticut, USA). The control conditions and procedure in the nanoprecipitation technique are briefly described. An organic solution (AC) containing 10 mg mL^{-1} of PLGA was injected into an aqueous solution of 5% of PVA (with an organic solvent fraction of 0.167), using a NE-300 Just Infusion™ Syringe Pump (New Era Pump Systems Inc, Farmingdale, New York, USA). After both, the emulsification and the nanoprecipitation, the control parameters used in the solvent evaporation and purification are as follows: the organic solvent was evaporated under magnetic stirring at 400 rpm, at room temperature. Then, PNP were

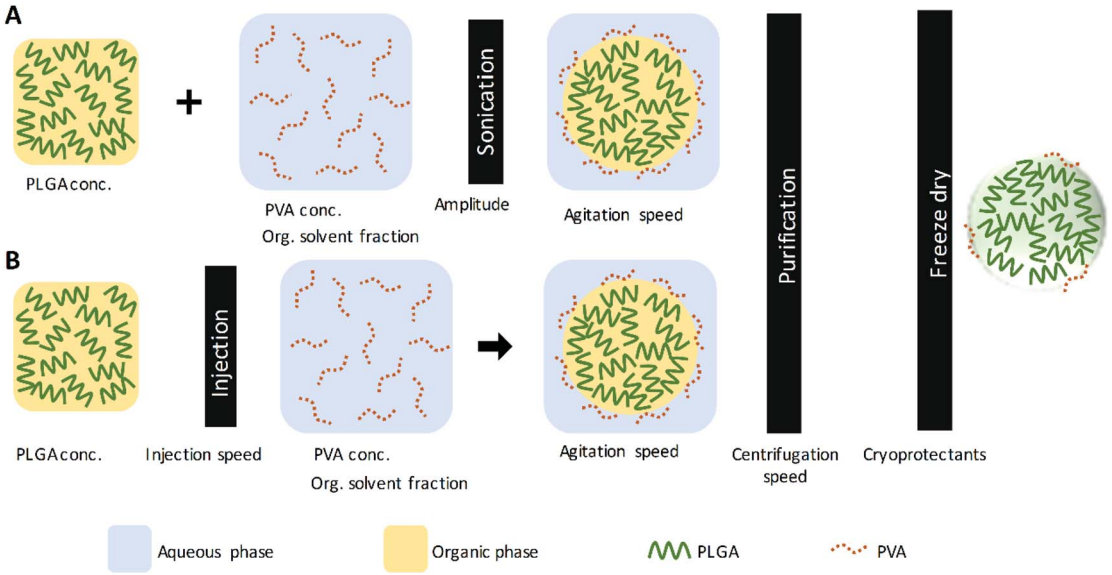

Fig. 1 Nanoparticle preparation scheme by (A) the single emulsification and (B) the nanoprecipitation techniques.

washed by three centrifugation cycles using a Sigma 3-30KS centrifuge (Sigma Laborzentrifugen GmbH Osterode am Harz, Germany) operated at 37 565 × *g* (20 000 rpm) for 20 minutes, discarding supernatant and resuspending the pellet nanoparticles in deionized water.

A cryoprotectant solution (sucrose, glucose or lactose) was added to the PNP solution and then placed into a freezer at −80 °C. Finally, PNP were freeze-dried in lyophilizer freezone 2.5 Liter Benchtop (Labconco, Kansas City, Missouri, USA). Experiments were performed by triplicate.

Nanoparticle characterization

Nanoparticle size, size distribution, and zeta potentials were measured using a Zetasizer Nano ZS equipment (Malvern Instruments Ltd., Worcestershire, United Kingdom). Measurements of PNP sizes were performed by dynamic light scattering (DLS). Refraction index used in the analysis was 1.33 and water was used as the dispersant. Each sample was measured three times with 10 runs respectively for size analysis. Zeta potential of each sample was measured by duplicated with at least 10 runs at constant temperature (25 °C) by laser Doppler electrophoresis. Size averages and zeta potentials were obtained from three independent experiments. All the DLS sizes, PDI, and zeta potentials were measured after purification unless noted. Surface morphology of PNP was analyzed by scanning electron microscopy (SEM) through a field emission scanning electron microscopy (Hitachi S-4800 FE-SEM, Hitachi Corporation, Tokyo, Japan). Samples were prepared by placing a small number of lyophilized nanoparticles on a double-sided carbon tape, previously placed on a SEM stub. Compressed air was used to remove loose nanoparticles. The platinum coating was applied using with an Anatech Hummer 6.2 sputter system (Anatech USA, Hayward, California, USA). A total of 60 seconds under 10 mA under argon plasma were applied. A beam strength of 1.0 kV and a working distance in the range of 8–9 mm were used to visualize nanoparticles.

Data analysis

Statistical analysis for behavioral experiments was carried out on PNP size, polydispersity index and zeta potential

Table 1 Formulation parameters analyzed in the nanoparticle preparations by the single emulsification and the nanoprecipitation techniques

Emulsification technique				Nanoprecipitation technique			
PLGA concentration (mg mL^{-1})	5	10	15	PLGA concentration (mg mL^{-1})	5	10	15
PVA concentration (%)	1	3	5	PVA concentration (mg mL^{-1})	1	3	5
Organic solvent fraction	0.50	0.33	0.167	Organic solvent fraction	0.50	0.33	0.167
Sonication amplitude (%)	25	50	75	Injection speed (mL min^{-1})	0.6	1.2	2.4
Speed of agitation in evaporation (rpm)	200	300	400	Speed of agitation in evaporation (rpm)	200	300	400
General analysis							
Purification [rpm (×*g*)]	10 000 (9391)			15 000 (21 130)			20 000 (37 565)
Cryoprotectant	Sucrose			Lactose			Glucose

measurements using R (ver. 3.0.1) with RStudio (ver. 1.2.1335). Results were analyzed by ANOVA followed by Tukey's HSD test ($\alpha = 0.05$ was used, unless otherwise indicated) comparing different parameters such as PLGA concentration, PVA concentration, organic and aqueous phase ratio, sonication and agitation speed for nanoparticles prepared by emulsification. In the same manner, parameters studied for nanoparticles prepared by nanoprecipitation were PLGA concentration, PVA concentration, organic and aqueous phase ratio, and agitation speed. Also, the effect of the use of different cryoprotectants was considered in the statistical analysis. When the *p*-values were minor or equal than 0.05, the differences were considered statistically significant.

Results and discussion

PLGA nanoparticles were prepared using two of the most commonly used techniques to encapsulate hydrophobic compounds: the single emulsification solvent evaporation and the nanoprecipitation. The most critical parameters were investigated during the fabrication of PLGA nanoparticles to evaluate their effects on the mean particle size, polydispersity index (PDI) and zeta potential (ζ).

PLGA concentration effects on the size of the PNP

The effect of PLGA concentration over the diameter size of nanoparticles prepared by the emulsification and nanoprecipitation techniques are presented in Fig. 2A. Three concentrations of P17A were used in the nanoparticle preparations: 5 mg mL^{-1}, 10 mg mL^{-1}, and 15 mg mL^{-1}. In this range of PLGA concentrations, no significant effect on the diameter size of PNP prepared by emulsification technique was observed, with diameters around 175 nm in all formulations ($p > 0.05$). Similarly, Xie *et al.*, reported no significant effects of PLGA concentration over the diameter size in nanoparticles prepared by the double emulsification-evaporation solvent technique.[52] In contrast, several authors report an increase in the particle size by increasing the polymer concentration.[53–56] This difference is probably due to the PLGA concentration study range, the effect of the PLGA copolymers, lactic acid, and glycolic acid on the size of the PNP, and the molecular weight of the PLGA.[57–59] In addition to molecular weight and co-polymer composition, PLGA can undergo several end-terminal modifications (such ester end-capping of its free carboxylic acid end-group) that affect the final physicochemical characteristics considerably.[60] The end group of PLGA is a factor that affects the hydrophilicity of the polymer,[61] PLGA with a final ester group is more hydrophobic than PLGA with a carboxyl group.[62] For the nanoprecipitation technique, the same three concentrations of P17A than for emulsification technique were used. In this case, the size of nanoparticles increased proportionally to the concentration of P17A, obtaining nanoparticles with average sizes of 157.0 ± 9.0 nm, 174.0 ± 0.33 nm, and 194.5 ± 2.61 nm, respectively to P17A concentrations of 5 mg mL^{-1}, 10 mg mL^{-1}, and 15 mg mL^{-1}; $p = <0.05$. A linear fit of experimental results correlates the PNP diameter size (D) with the concentration of

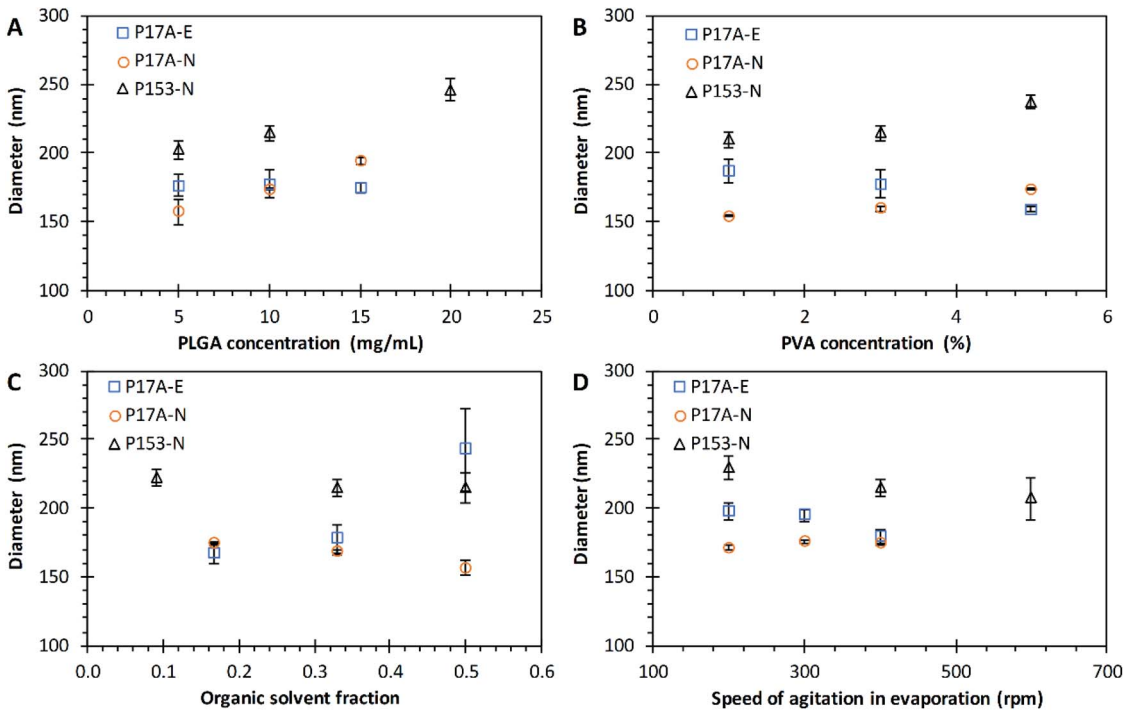

Fig. 2 Effect of varying formulation parameters on nanoparticle diameter size. (A) PLGA concentration; (B) PVA concentration; (C) organic solvent fraction; and (D) speed of agitation in evaporation. Preparations by the emulsification technique with PLGA of 17 kg mol^{-1}, P17A-E (□). Preparations by the nanoprecipitation technique with PLGA of 17 kg mol^{-1}, P17A-N (○), and PLGA of 153 kg mol^{-1}, P153-N (Δ). Data represent mean ± SD ($n = 3$).

P17A in the organic solvent (C_{P17A}) following the equation $D = 3.7511C_{P17A} + 137.69$, with an excellent coefficient of determination ($R^2 = 0.9971$). This equation could help to tune the diameter size of nanoparticles of P17A prepared by nanoprecipitation. In addition, the size increment of PNP regarding the polymer concentration could be related to the phenomenon of super-saturation, which is important for the nucleation process, as discussed in the literature.[63] Other authors explain that an increase in the viscosity of the organic phase means more polymer is contained in the drops formed during the nanoprecipitation process, leading to larger PNP.[3,64] The nanoprecipitation technique was also employed to prepare nanoparticles with the polymer P153. The results were similar to the ones obtained by nanoprecipitation with P17A polymer; the size of the nanoparticles increase by increasing the concentration of P153 (C_{P153}). The average diameter values were 202.5 ± 6.84 nm, 214.8 ± 5.60 nm, and 246.3 ± 7.51 nm, respectively to C_{P153} of 5 mg mL^{-1}, 10 mg mL^{-1}, and 20 mg mL; $p = <0.05$. A linear fit of this data results in the equation $D = 2.952C_{P153} + 186.76$, with an excellent R^2 of 0.9968; showing that is possible to tune the diameter of P153 nanoparticles in function of C_{P153}. These results indicate that the amount of PLGA plays an important role in the final size of PNP prepared by the nanoprecipitation technique. Also, the diameter size of PNP prepared by this technique could be tuned in function of the PLGA concentration used in the formulation. In contrast, the emulsification technique do not show a significant effect of the concentration of PLGA over the diameter size of PNP in the range studied.

PVA concentration effects on the size of the PNP

Another parameter considered during the PLGA nanoparticle preparations was concentration of PVA in the aqueous phase. Aqueous solutions of PVA of 1%, 3%, and 5% were used for the preparation of PNP in both techniques. The amount of surfactant plays an essential role in the emulsification-solvent evaporation process, by the protection of the droplets containing the PLGA against coalescence.[65,66] Fig. 2B illustrates the effect of PVA concentration (C_{PVA}) on the particle size for PNP prepared by both techniques. In the emulsification technique, the PNP sizes decreased as the C_{PVA} increased, with average diameter values of 187.0 ± 8.5 nm, 177.7 ± 1.6 nm, and 159.1 ± 2.0 nm, correspondingly to C_{PVA} of 1%, 3%, and 5%. However, this results are not statistically significant ($p = 0.051$), probably to the number of repetitions. Nevertheless, a trendline analysis of the experimental results indicate a fair linear fit with the equation $D = -6.975C_{PVA} + 195.53$ ($R^2 = 0.9643$). Miladi *et al.* found that the particle size decreases from 301 nm to 255 nm, when the PVA concentration increased from 0.25% to 1%, respectively.

They explained this result by the increased in the viscosity of the aqueous phase after the augment in the PVA concentration.[67] Therefore, the decrease in the size of the PNP obtained in this work is probably due to the difference in the stability of the emulsion, formulated with different concentrations of PVA. Kejdušová *et al.* reported that an increase in the concentration of PVA guarantees a better stabilization of the system; hence, a decrease in the coalescence of the emulsion.[66] Since PNP are forming from the emulsion droplets after solvent evaporation, its size depends on the size and stability of these droplets.[68] Also, according to Sahoo *et al.* at concentrations lower than 2.5% w/v of PVA, this one exists as a single molecule in solution, and above this concentration, PVA exists as an aggregated form and has an enhanced surfactant activity. Besides, they found that the residual PVA associated with the nanoparticles increased by increasing the miscibility of the solvent with water.[69] Therefore, droplets formed during emulsification would be more stable, resulting in smaller PNP. On the other hand, it was found that by using P17A in the nanoprecipitation technique, PNP sizes increased as the C_{PVA} increases, with average diameter values of 154.5 ± 0.76 nm, 159.8 ± 1.85 nm, and 174.0 ± 0.33 nm, regarding to C_{PVA} of 1%, 3%, and 5%, with statistically significant differences ($p < 0.05$). A fair linear fit of this data comes with the equation $D = 4.8917C_{PVA} + 148.09$ ($R^2 = 0.9352$). Similar results in the nanoparticle size when varying the C_{PVA} were obtained by using P153 with the nanoprecipitation technique (Fig. 2B). The PNP sizes increased as C_{PVA} increased ($p < 0.05$). In addition, a reasonable linear fit of the data could be observed, with the equation $D = 6.835C_{PVA} + 200.16$ ($R^2 = 0.8803$). These observed tendencies of PNP size increments by increasing the C_{PVA} in the nanoprecipitation technique could be due to PVA deposited on the surface of the PNP, as reported in previous works.[70] In agreement, Murakami *et al.*, found that a certain amount of PVA remained adsorbed on the surface of the PLGA nanoparticles after the washing steps.[71] Also, Badri *et al.* report similar results, they found that the augment of PVA, increased the particle size from 169 nm to 283 nm.[22] Different tendencies in the size of nanoparticles were obtained between both techniques when the C_{PVA} increased, finding that in the emulsification technique the size of PNP decreased, while in the nanoprecipitation technique the size of PNP increased. This difference could be because in the emulsification technique the stability of the emulsion is a critical step in the formation of the nanoparticle.[72]

Organic solvent fraction effects on the size of the PNP

The effect of organic solvent fraction (F_{os}) on the diameter size of the PNP prepared by the emulsification and nanoprecipitation techniques was evaluated. The polymer P17A was used in emulsification and nanoprecipitation; additionally, the polymer P153 was evaluated by the nanoprecipitation technique. The outcome of F_{os} over the diameter of PNP for both techniques is presented in Fig. 2C. An increase in the PNP diameter size with an increment of the F_{os} was observed in the emulsification technique (with P17A), with diameters of 167.5 ± 7.8 nm, 177.7 ± 10.6 nm, and 242.8 ± 30.0 nm, correspondingly to F_{os} of 0.167, 0.330, and 0.500, these results were statistically significant ($p < 0.05$). However, a poor linear fit of this data comes with the equation $D = 227.25F_{os} + 120.48$ ($R^2 = 0.8581$). Other authors report similar results, for example, Habib *et al.*, found that the size of the nanoparticles decreased when using acetone, with F_{os} values from 0.330 to 0.167.[73] Also, a study with nanoparticles of mPEG-PLGA prepared by

emulsion solvent evaporation reported that as the F_{os} increased, the system reduced the net shear stress due to a constant external energy input, which led to the increased size of the nanoparticles.[74] The organic solvent fraction in the emulsification technique played an important role in the resulting PNP sizes. On the other hand, the evaluation of the F_{os} used in nanoprecipitation with P17A and P153 (Fig. 2C), shows that the size of the PNP decreased as F_{os} increased. The average diameter sizes values of PNP prepared with P17A were of 174.0 ± 0.3 nm, 167.8 ± 1.3 nm, and 156.6 ± 5.5 nm, respectively to the F_{os} of 0.167, 0.330, and 0.500; ($p < 0.05$). Also, a good linear fit of this data results in the equation $D = -52.346F_{os} + 183.54$ ($R^2 = 0.9786$), showing that is possible to tune the diameter of P17A nanoparticles in function of F_{os}. Additionally, the average diameter sizes values of PNP prepared with P153 were 227 ± 6.1 nm, 214.8 ± 5.6 nm, and 214.6 ± 11.2 nm, correspondingly to F_{os} of 0.090, 0.167, and 0.500. Nevertheless, the statistical analysis did not show a significant difference between the range of F_{os} used ($p > 0.05$), possibly for the number of repetitions. The effect of the organic solvent fraction in the nanoprecipitation technique has been reported lately in the literature.[75,76] Chaudhary *et al.* reported smaller cefixime loaded PLGA nanoparticles when the organic solvent fraction decreased, using a modified precipitation method; attributing this size reduction to the coalescence prevention.[77] Also, de Oliveira *et al.* found that the mean particle size decreased when the organic solvent fraction decreased; if the size reduction was a result of the formation of a higher number of nucleation sites. This increase in the nucleation sites consequently leads to the generation of smaller particles.[78] The nature of the organic solvent is also an important factor when manufacturing PNP *via* nanoprecipitation. The organic solvent should dissolve the polymer as well as miscible with water.[79] Hence, other authors have studied the effect of the miscibility of the organic solvent in water. Cheng *et al.*, report that an increase of water miscibility led to a decrease in the average docetaxel-loaded PEGylated PLGA nanoparticle size, which is presumably due to more efficient solvent diffusion and polymer dispersion into water.[80] Also, Huang and Zhang report that solvents with a high diffusion coefficient favor the formation of smaller PNP with the narrower distribution.[81] Therefore, it can be highlighted that the effect of the size of the PNP, depends not only on the range of study but also of the nature of the organic and aqueous phases used. Almoustafa *et al.* advises that choosing the solvent is the primary step in size tuning and encapsulation efficiency for the nanoprecipitation technique.[20] Moreover, in the case of PNP with and encapsulated drug, the effect of the organic solvent fraction in particle size also depends on the solubility of the drug in the external phase.[82]

Speed of agitation effects on the size of the PNP

The effects of speed of agitation (A_{rpm}) on the solvent evaporation over the diameter size of PNP prepared by the emulsification and nanoprecipitation techniques are presented in Fig. 2D. The PNP prepared by the emulsification technique with P17A were agitated at 200 rpm, 300 rpm, and 400 rpm, resulting in average diameter values of PNP of 198.2 ± 6.1 nm, 195.0 ± 4.1 nm, and 179.4 ± 5.2 nm, respectively. This results are statistically significant ($p < 0.05$); however only a reasonable linear fit of this data was found, resulting in the equation $D = -0.0939A_{rpm} + 219.06$ ($R^2 = 0.8745$). In analogous way, for the nanoprecipitation technique (P17A), the same three agitation speeds were evaluated, obtaining PNP with average diameter sizes of 171.4 ± 1.6 nm, 175.7 ± 1.7 nm and 174.0 ± 0.3 nm, respectively to speed of agitation of 200 rpm, 300 rpm, and 400 rpm; ($p < 0.05$). Despite the results are statistically significant, the diameter values were in a very close range; also, a bad linear fit of this data was found (not reported). Furthermore, in the same technique but using P153, the PNP diameter sizes resulted in 229.5 ± 8.3 nm, 214.8 ± 5.6 nm, and 207.0 ± 15.6 nm for 200 rpm, 300 rpm, and 600 rpm, respectively (Fig. 2D), with significant effects of the agitation ($p < 0.05$). A good linear fit of this data results in the equation $D = -0.0562A_{rpm} + 239.57$, with R^2 of 0.9705. Malkani *et al.*, found that the agitation speed in the nanoprecipitation process had influence in the particle size of the celecoxib nanosuspension. This could be due to faster evaporation of the organic solvent, increasing the rate of drug precipitation and resulting in larger particles.[83] Also, Lince *et al.*, explain that the speed of agitation influences the nucleation speed of the polymer, where poor mixes result in slow nucleation speeds, generating larger particles; while proper mixing promotes the increase of the nucleation speed, leading to the formation of small particles.[63] During the evaporation of the solvent, the surface hardening of the nanoparticles takes place.[84] Therefore, the A_{rpm} is an essential parameter in the formation of nanoparticles. In the range of speed of agitation studied for both techniques, emulsification and nanoprecipitation, the PNP size tend to decrease as the speed of agitation in the solvent evaporation increase.

PLGA concentration effects on the PDI of the PNP

The effects of PLGA concentration over the polydispersity index of PNP were evaluated in both techniques, emulsification and nanoprecipitation (Fig. 3A). The PLGA concentration did affect the PDI average value in the emulsification technique, with values of 0.140 ± 0.066, 0.110 ± 0.004, and 0.097 ± 0.024 when the P17A concentration increased from 5 mg mL^{-1}, 10 mg mL^{-1}, and 15 mg mL^{-1}, respectively; in the three cases indicating a homogeneous size distribution. However, according to the statistical analysis, this differences are not significant ($p > 0.05$), probably indicating that a major number of repetitions are needed. Dangi and Shakya also found that the PDI was reduced by increasing the concentration of PLGA from 0.5 to 1.0.[85] In addition, in this range of study, the P17A concentration have a significant effect on the PDI with the nanoprecipitation technique. The resulting values of PDI were 0.067 ± 0.005, 0.048 ± 0.002, and 0.041 ± 0.009 for P17A concentrations of 5 mg mL^{-1}, 10 mg mL^{-1}, and 15 mg mL^{-1}, respectively ($p < 0.05$). These PDI were smaller than the ones obtained by the emulsification technique, indicating a narrow distribution size and the

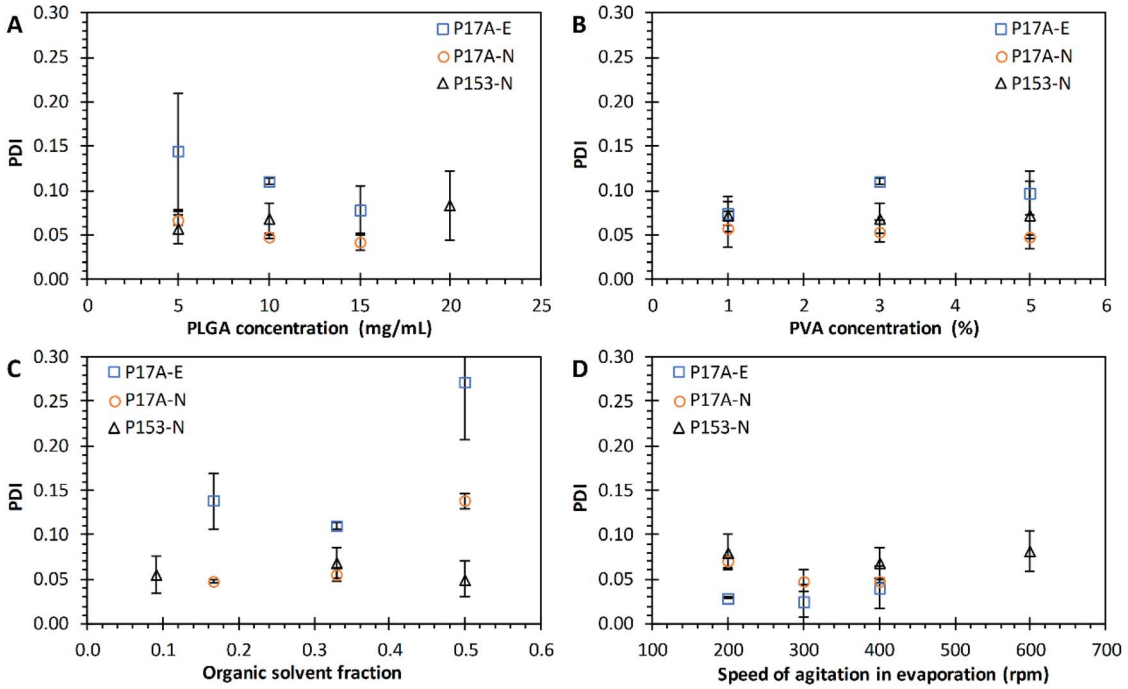

Fig. 3 Effect of varying formulation parameters on nanoparticle PDI. (A) PLGA concentration; (B) PVA concentration; (C) organic solvent fraction; and (D) speed of agitation in evaporation. Preparations by the emulsification technique with PLGA of 17 kg mol^{-1}, P17A-E (□). Preparations by the nanoprecipitation technique with PLGA of 17 kg mol^{-1}, P17A-N (○), and PLGA of 153 kg mol^{-1}, P153-N (Δ). Data represent mean ± SD (n = 3).

formation of uniform and homogeneous PNP for all formulations. Also, a fair linear fit comes with the equation PDI = $-0.0026C_{P17A} + 0.078$ ($R^2 = 0.9297$). The same effect of PDI over the nanoprecipitation technique was observed when P153 was used, obtaining a maximum value of PDI of 0.08, but with no statistical significances ($p > 0.05$). The results presented in the Fig. 3A, for both techniques, emulsification and nanoprecipitation, shown a slight trend to decrease the PDI values as increasing the concentration of PLGA.

PVA concentration effects on the PDI of the PNP

The effects of PVA concentration over the PDI of PNP were evaluated in both techniques, emulsification and nanoprecipitation, and are presented in Fig. 3B. The PNP average values of PDI obtained from the emulsification technique (P17A) were 0.074 ± 0.013, 0.111 ± 0.004, and 0.097 ± 0.002, corresponding to PVA concentrations of 1%, 3%, and 5%. However, the statistical analysis shows that an increase in PVA concentration does not show a significant effects on the final PDI ($p > 0.05$). Similarly, for the nanoprecipitation technique, with P17A and P153, the PDI values did not show variations in the range of PVA concentrations evaluated, obtaining PDI values around 0.05 ($p > 0.05$), and PDI values around 0.07 ($p > 0.05$), respectively. The solubility, viscosity, and surface tension of PVA vary in function of the temperature, concentration, % hydrolysis, and molecular weight of this polymer.[86] In this context, several authors report that the degree of hydrolysis and the molecular weight of PVA have influence the PNP size, and the PNP polydispersity index.[87–90]

Organic solvent fraction effects on the PDI of the PNP

Fig. 3C presents the effect of F_{os} over the PDI values for the emulsification and the nanoprecipitation techniques. The resulting PDI values from the emulsification technique (P17A) were 0.138 ± 0.031, 0.111 ± 0.004, and 0.272 ± 0.064, corresponding to the F_{os} of 0.167, 0.330, and 0.500. These PDI values indicate that F_{os} affects directly to the monodispersity of the PNP ($p < 0.05$). Comparable, for the nanoprecipitation technique with P17A, the PDI values increased as the F_{os} increased, getting values of 0.048 ± 0.002, 0.056 ± 0.008, and 0.138 ± 0.008, for F_{os} of 0.167, 0.330, and 0.500, respectively ($p < 0.05$). In addition, when using P153 polymer and the nanoprecipitation technique, the average PDI values ranged between 0.05, and 0.07 for all the formulations, which indicates a narrow size distribution. Nevertheless, the statistical analysis of this data show no dependency of F_{os} with the PDI ($p > 0.05$). Despite all the values obtained show monodispersed PNP systems, the data obtained with both techniques and the two polymers were poorly fitted into a linear curve (data not shown).

Speed of agitation effects on the PDI of the PNP

The effects of A_{rpm} on the solvent evaporation over the PDI of PNP prepared by the emulsification and nanoprecipitation techniques are presented in Fig. 3D. The PDI values obtained from the emulsification technique (P17A) were found between 0.03 and 0.04 for the range of A_{rpm} studied, indicating a narrow size distribution, but with no significant differences ($p > 0.05$). Narayanan *et al.*, reported that hyaluronidase loaded PLGA nanoparticles size is reduced due to shear stress, where PVA

could participate stabilizing the reduced particles and preventing the formation of aggregates.[91] The results of PDI obtained from the nanoprecipitation technique (P17A) also presented low PDI values, indicating narrow size distributions. In this case, the data resulted in significant differences ($p < 0.05$) but resulted in a poor fit to a linear behavior (data not shown). Similarly, the PDI values obtained with the nanoprecipitation technique, but using the polymer P153, shown narrow size distributions for all the A_{rpm} studied, but with no significant differences ($p > 0.05$). Despite no trends were obtained with the A_{rpm} over the PDI of PNP, is notable that all formulations presented narrow size distributions.

PLGA concentration effects on the ζ of the PNP

The effects of PLGA concentration over the ζ of PNP for both techniques were evaluated (Fig. 4A). The ζ values of PNP prepared by the emulsification technique ranged between −26.8 mV and −30.0 mV for all the P17A concentrations evaluated ($p > 0.05$). This negative charge was due to the presence of terminal carboxylic groups (–COOH) on the surface of nanoparticles.[92,93] Similar results were obtained for the nanoprecipitation technique, with ζ values of PNP in the range of −20.8 mV and −23.4 mV for all the P17A concentrations evaluated ($p < 0.05$). Moreover, when using the same nanoprecipitation technique but with P153, the ζ values were in the range of −5.0 mV and −5.9 mV. The considerable difference in the ζ results between the formulations with P17A and P153 it is due to the polymers termination groups, which are acid terminated, and ester terminated, respectively. It should be mentioned that the anionic nature that PLGA gives to the nanoparticles also depends on its molecular weight and concentration.[94,95]

PVA concentration effects on the ζ of the PNP

Fig. 5C presents the ζ of PNP obtained with different C_{PVA} for both techniques, emulsification and nanoprecipitation. The ζ for the emulsification technique (P17A) shows an increase as the C_{PVA} increase, with values of −29.4 ± 6.8 mV, −26.8 ± 5.0 mV, and −26.6 ± 5.5 mV, for C_{PVA} of 1%, 3%, and 5%, respectively; however, these values do not present statistical differences ($p > 0.05$). Prabha and Labhasetwar reported that PVA attached to the surface nanoparticle affects the charge since the nanoparticles with the highest amount of PVA associated with the surface, presented a decrease in their anionic charge.[96] In the case of the nanoprecipitation technique (P17A), the ζ decreased as the C_{PVA} increased. The ζ values are −15.0 ± 1.0 mV, −18.3 ± 3.1 mV, and −23.4 ± 1.7 mV, corresponding to C_{PVA} of 1%, 3%, and 5%. The influence of C_{PVA} over the ζ is statistically significant, with a $p < 0.05$; also, a good linear fit could be obtained with the equation $\zeta = -2.1028C_{PVA} - 12.566$ ($R^2 = 0.9851$). In addition, the ζ that results from the nanoprecipitation technique when the polymer P153 was used ranged from −3.7 mV to −6.0 mV ($p > 0.05$). As mentioned above, the differences in PNP ζ between the formulations with P17A and P153 are due to the terminations groups of PLGA.

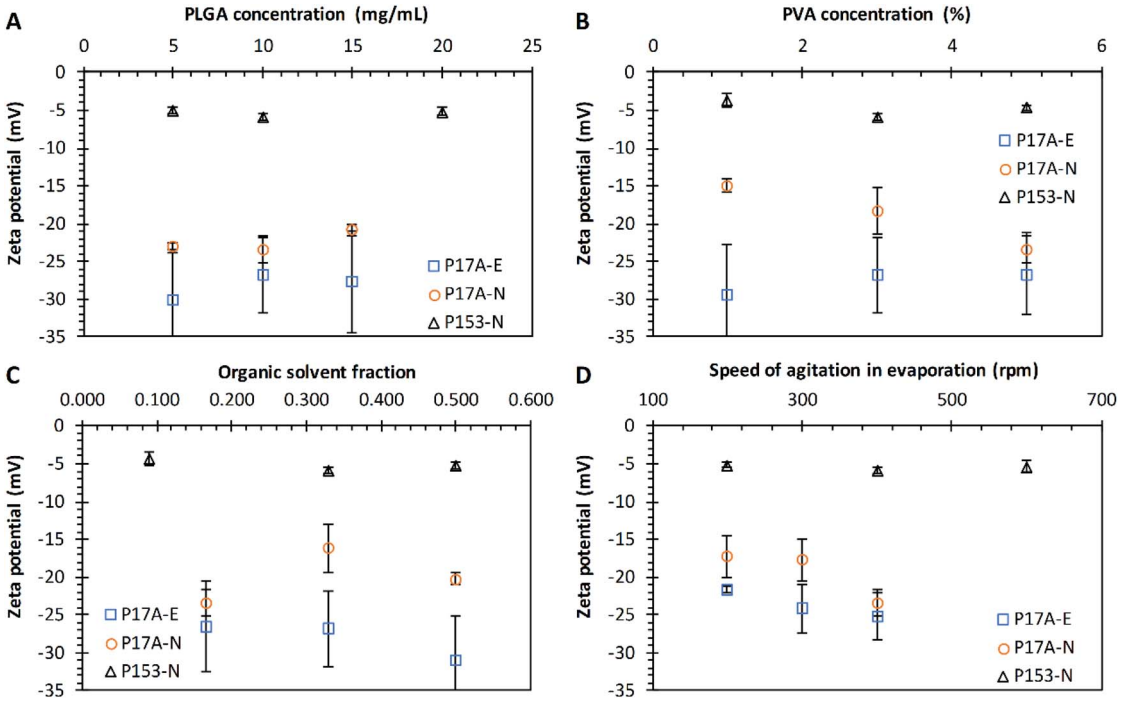

Fig. 4 Effect of varying formulation parameters on nanoparticle zeta potential. (A) PLGA concentration; (B) PVA concentration; (C) organic solvent fraction; and (D) speed of agitation in evaporation. Preparations by the emulsification technique with PLGA of 17 kg mol^{-1}, P17A-E (□). Preparations by the nanoprecipitation technique with PLGA of 17 kg mol^{-1}, P17A-N (○), and PLGA of 153 kg mol^{-1}, P153-N (Δ). Data represent mean ± SD ($n = 3$).

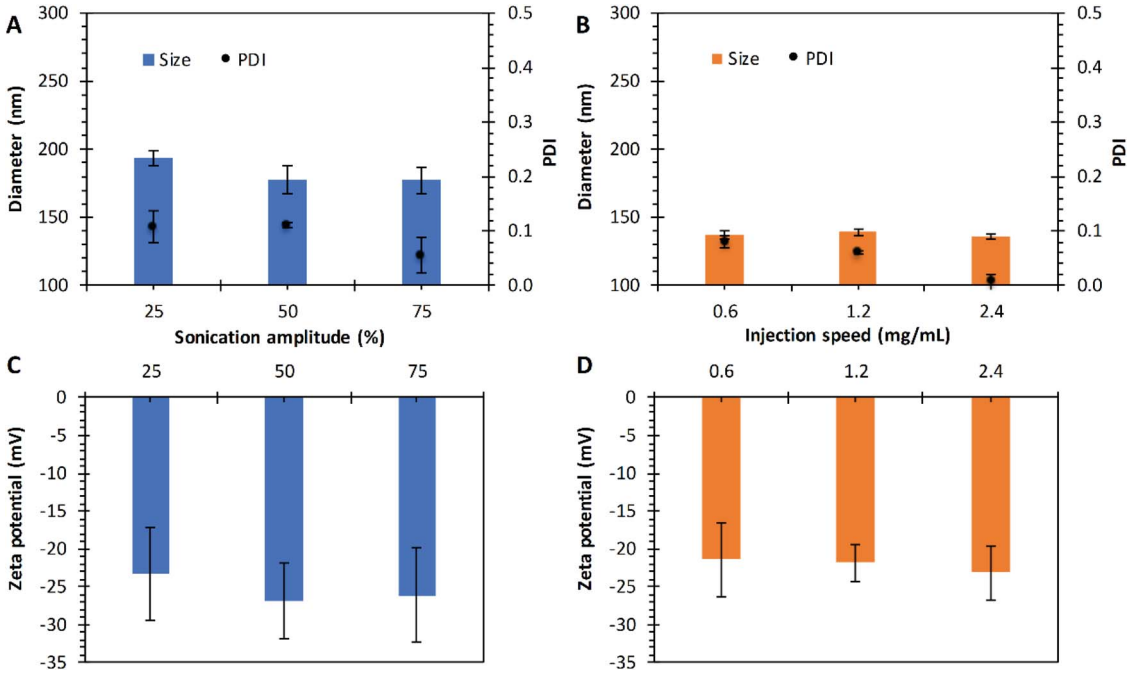

Fig. 5 Effect of sonication amplitude and injection speed on nanoparticles prepared by the emulsification and nanoprecipitation techniques, respectively. Diameter size and PDI as function of sonication amplitude (A), and the injection speed (B). Zeta potential as a function of the sonication amplitude (C), and the injection speed (D). Preparations made with PLGA of 17 kg mol^{-1}. Data represent mean ± SD (n = 3).

Organic solvent fraction effects on the ζ of the PNP

The effects of F_{os} over the ζ of PNP for both techniques were evaluated and the results are presented in Fig. 4C. The ζ values obtained in the emulsification technique with P17A ranged between −26.5 mV and −31.0 mV for all the F_{os} evaluated (p > 0.05). Also, the ζ values with the same polymer but with the nanoprecipitation technique ranged between −16.2 mV and −23.4 mV for the same range of F_{os} (p < 0.05). Despite the statistical differences, no good linear fit was found with this data. Also, Fig. 4C shows that when the polymer P153 with the nanoprecipitation technique was used, the ζ values ranged between −4.4 mV and −5.9 mV (p > 0.05). The differences are consistent with the terminations groups of PLGA used in the preparations, as discussed in previous sections.

Speed of agitation effects on the ζ of the PNP

The effect of the A_{rpm} in the evaporation of the organic solvent over the ζ of PNP was evaluated for both techniques; emulsification and nanoprecipitation, as presented in Fig. 4D. The ζ values obtained with the polymer P17A in the emulsification technique ranged between −22 mV and −25 mV for all the A_{rpm} evaluated (p < 0.05). A fair linear fit was found with the equation $D = -0.0169A_{rpm} - 18.571$ ($R^2 = 0.9353$). The ζ results obtained with the nanoprecipitation technique and the P17A polymer ranged between −17.3 mV and −23.4 mV for all the A_{rpm} evaluated (p < 0.05); however the results not present a good linear fit (results not shown). In the nanoprecipitation technique with P153, the ζ values were between −5.2 mV and −5.9 mV. These values were not significantly affected by the agitation (p > 0.05).

Sonicator amplitude and injection rate effects

The sonication amplitude was evaluated in the emulsification technique with P17A; where three different sonication amplitudes were used: 25%, 50%, and 75% corresponding to 30 μm, 60 μm, and 90 μm of amplitude. The PNP sizes obtained at different amplitudes are presented in Fig. 5A. Particle with average diameters of 193.4 ± 5.4 nm, 177 ± 10.6 nm, and 177 ± 10.0 nm were obtained for amplitudes of 25%, 50%, and 75%, respectively. The average PDI values obtained for 25% and 50% amplitude were 0.11, and it decreases to 0.05 when sonication was set at 75%, although not statistical significance was found for the diameters (p > 0.05), probably due to the use of an ice bath and short sonication periods. Literature reports that by increasing the power and duration of sonication, a reduction in the mean diameter of the nanoparticles is obtained, and the particle population distribution could change from bimodal to unimodal.[97,98] This effect can be attributed to the fact that the emulsion is carried out under high shear stress, which reduces the size of the emulsion droplets, correlating directly to the final size of the nanoparticles.[99]

In the nanoprecipitation technique with P17A, the injection speed was adjusted to 0.6 mL min^{-1}, 1.2 mL min^{-1}, and 2.4 mL min^{-1}. The diameters obtained ranged between 135 nm and 139 nm, with PDI ranging between 0.01 and 0.08, as depicted in Fig. 5B. Therefore, no variation is appreciated within the range of study (p > 0.05). Reports in the literature suggest that the resulting nanoparticle size can be predicted by the diffusion coefficient of solvent in water with the presence of the polymer, and explain that the organic solvent injection speed only affects

the rate of mass transport, but not the diffusion coefficient of the solvent.[81] In the present study varying the sonication amplitude and injection rate, PLGA acid terminated was used in both techniques, emulsion, and nanoprecipitation. This comparison can be noticed by comparing the zeta potential of both methods where surface charge values ranged between −21 mV and −27 mV for both techniques (Fig. 5C and D).

Purification process

The nanoparticle purification step follows the solvent evaporation in both techniques (emulsification and nanoprecipitation), removing the excess of PVA. Several methods of purification can be used, but centrifugation is practical to perform on small scale experiments.[100,101] In this work, three different centrifugation speeds were tested, 10 000 rpm (9391 × *g*), 15 000 rpm (21 130 × *g*), and 20 000 rpm (37 565 × *g*). For this study, the particles were prepared by the technique of emulsification with the following conditions, 10 mg mL^{-1} of P17A in the organic phase, 5% of C_{PVA}, 0.167 of F_{os}, 400 of A_{rpm}, and 75% of sonication amplitude. These nanoparticles were used as a model to evaluate the purification process. In summary, an increase in the overall size of the nanoparticles was consistent across the centrifugation cycles used in the purification, where the PNP had an overall increase of 56 nm, 30 nm, and 16 nm, as the centrifugation speed increased to 10 000 rpm, 15 000 rpm, and 20 000 rpm, respectively (Fig. 6A). Katas *et al.*, explain that centrifugation could increase particle size by the compaction of the particles due to high-speed spinning and, therefore, forming aggregates.[102] However, when the PNP were centrifuged, the PVA adsorbed on the surface could be washed more efficiently at 20 000 rpm of centrifugation, thus explaining the drop in PNP size following this washing, compared with centrifugation at 10 000 rpm, and 15 000 rpm. Variations on the PDI through the purification process indicates the presence of a non-uniform population of PNP. For the experiments performed at 10 000 rpm and 15 000 rpm, the PDI values start at 0.15 on the prewash measurement, along with the process, they increased, and at the end, the PDI values were 0.22 and 0.27 respectively. However, when purification was performed at 20 000 rpm, the PDI value decreased from 0.15 to 0.04, representing a monodisperse population of PNP. As mentioned above, when centrifugation speeds of 20 000 rpm are used, the purification of the PNP becomes more efficient, decreasing the PDI of nanoparticles. On the other hand, zeta potential decreased in the progression of the purification cycles for all preparations (Fig. 6B). The values decreased from −16 mV to −28 mV corresponding to the prewash and the third cycle, respectively, when purifying at 10 000 rpm. Similarly, values decreased from −15 mV to −31 mV from prewash to the third cycle, respectively, when purifying at 15 000 rpm; and from −15 mV to −34 mV from prewash to the third cycle, respectively, when purifying at 20 000 rpm (Fig. 5B). This effect could be attributed to the removal of the PVA layer on the surface of the nanoparticles as the purifying process is carrying out. By removing the PVA layer, the carboxyl groups from the PLGA become exposed and the surface charge is altered.[103,104]

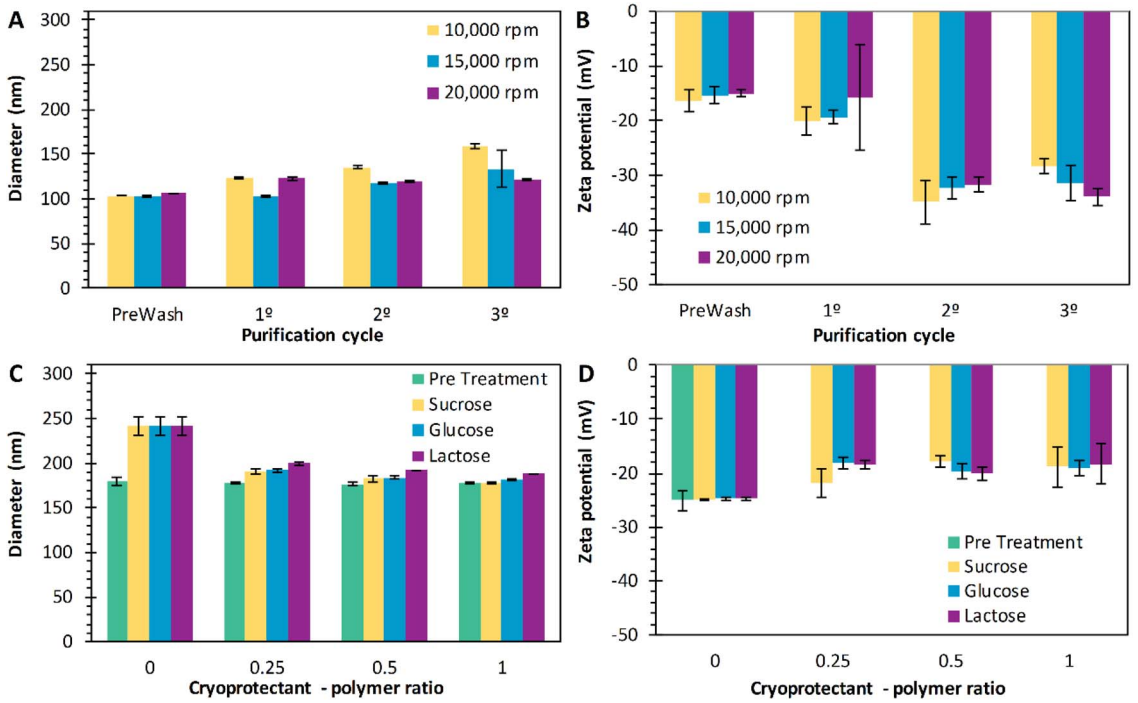

Fig. 6 Diameter size (A) and zeta potentials (B) of nanoparticles after the centrifugation cycles at 10 000 rpm (9391 × *g*) (■), 15 000 rpm (21 130 × *g*) (■), and 20 000 rpm (37 565 × *g*) (■). Diameter size (C) and zeta potentials (D) of PLGA nanoparticles when different cryoprotectant – polymer ratios were used: pre-treatment (■), sucrose (■), glucose (■), and lactose (■). Data represent mean ± SD ($n = 3$).

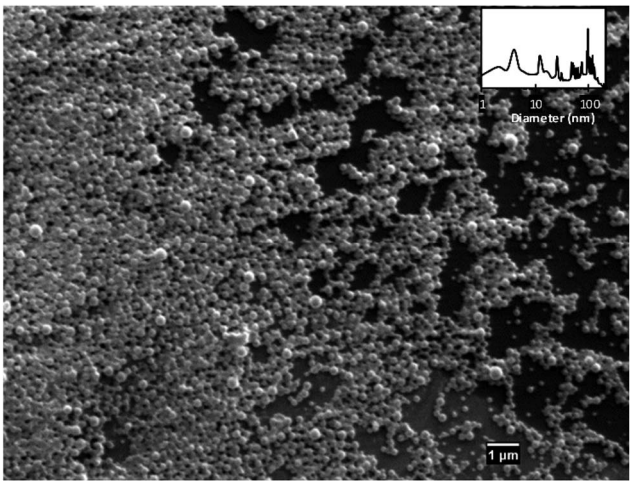

Fig. 7 Scanning electron micrograph of PLGA nanoparticles.

Cryoprotectants

The final part of the PNP preparation is freeze drying. During this stage, the use of cryoprotectants is commonly used to prevent nanoparticles from aggregation. Authors have used sugars such as trehalose, sucrose, lactose, glucose, and mannitol as cryoprotectants while freeze-drying nanoparticles.[105,106] These sugars affect the glass transition temperature, and allow a high redispersion speed, and stabilization upon storage.[107] Holzer *et al.* evaluated the effect of sucrose, trehalose, and mannitol on the storage stability of PNP.[108] In the present work, the effect of sucrose, glucose, and lactose at different ratios (0 : 1, 0.25 : 1, 0.5 : 1 and 1 : 1) concerning initial mass of PLGA were evaluated. The diameter size, PDI and ζ of the PNP were measured before and after the lyophilization process. Before lyophilization, it was found that the sizes of the PNP were not affected by the addition of the cryoprotectants ($p > 0.05$); however, the ζ did change (Fig. 6D). For sucrose, from -25 mV to -18 mV, glucose changed from -25 mV to -22 mV and lactose from -25 mV to -19 mV. Rampino *et al.*, report that the mechanism by which sugars protect particles resides in the interaction with the solute *via* hydrogen bonding.[109] Therefore, the decrease of the zeta potential could be explained, by the coverage of the surface of the PNP. Besides, the PDI was maintained between 0.02 and 0.04 for all preparations, indicating a homogeneous size distribution. After lyophilization, the PNP were resuspended in water, and their size (Fig. 6C) and zeta potential (Fig. 6D) were measured again. When sucrose was added, PNP diameters of 190.4 nm, 183.3 nm, and, 178.3 nm were obtained for mass ratios of 0.25 : 1, 0.5 : 1, and 1 : 1, respectively; glucose had a similar result for the same ratios, with PNP sizes of 193 nm, 184.3 nm, and 182.1 nm, respectively. Similarly, as the mass ratio of lactose incremented, the size resulted in values of 200 nm, 193 nm, and 189 nm for mass ratios of 0.25 : 1, 0.5 : 1, and 1 : 1, respectively. According to the statistical analysis, these are all significant changes in size, with values of p limiting with zero, for $\alpha = 0.001$, for the three cryoprotectants used. Also, when sucrose was used, the PDI values of 0.21, 0.11, 0.07, and 0.04 were obtained for the mass ratios of 0, 0.25, 0.5, and 1, respectively ($p < 0.05$). Similarly, for the glucose and the lactose, the PDI values decreased as the mass ratio of cryoprotectant increased, with values of $p < 0.05$. Tang and Shapiro reported smaller PNP average sizes with the addition of cryoprotectants, attributing the results to the ability of sugar additive to form a glassy amorphous matrix around the particles, preventing the particles from sticking together during the water removal.[110]

Also, Saez *et al.*, discuss that the addition of cryoprotective agents makes the frozen mass behave more as fluid than a solid and it provides better mechanical protection of the PNP. Consequently, PNP aggregation or any alteration due to the pressure developed by the growth of crystals is avoided.[111] Besides, all the zeta potential values decreased when the cryoprotectants were added (Fig. 6D), compared to the particles without cryoprotectants, with significant results for the use of sucrose ($p = 0.004$) and glucose ($p = 0.044$); but not significant for the use of lactose ($p = 0.060$).

Surface morphology

The morphological characteristics of dried PNP were determined by SEM analysis, showing a regular spherical shape and smooth surface. Fig. 7 shows the micrograph of PLGA nanoparticles prepared by emulsification technique with the following conditions: 10 mg mL^{-1} of PLGA in the organic phase, 5% of C_{PVA}, F_{os} of 0.167, A_{rpm} of 400 rpm, 75% of sonication amplitude and 20 000 rpm of centrifugation speed. The histogram analysis of Fig. 7 (inset) obtained by the software Image J 1.8.0_112 (counting more than 200 particles) shown a diameter of 87 $\pm$ 40 nm. The diameter obtained from the micrograph is in concordance with the diameter sizes reported by DLS analysis (177.7 $\pm$ 10.6 nm); this by comparing those hydrodynamic diameters in solution to the diameters measured under drying conditions in SEM. Similar images could be obtained for all the preparations.

Conclusions

A systematic study presenting the effects of the primary formulation parameters involved in the preparation of PLGA nanoparticles, *via* the emulsification technique and the nanoprecipitation technique is presented. The PLGA concentration, PVA concentration, organic solvent fraction, and agitation speed were evaluated in both techniques. Also, in the emulsion technique was evaluated the sonication amplitude; w in the nanoprecipitation technique, the organic phase injection velocity was studied. Additionally, the purification process, the use of cryoprotectants, and the surface morphology were studied. It was found that polymer concentration, as well as types of polymer-terminated chain, have significant influence regarding the physicochemical characteristics evaluated (size, PDI, and zeta potential). The particle size could be controlled by the PLGA concentration and PVA concentration in the nanoprecipitation technique. While in the emulsification technique, the sizes could be controlled by the organic solvent fraction. For

both techniques, the use of high velocities of agitation in the evaporation of the solvents decreases the average diameter size. Also, by increasing the concentration of PLGA a slight decrease the PDI values can be achieved. Also, the ζ is not significantly affected by the variables explored; but the termination of PLGA polymer affects these values significantly. The centrifugation, lyophilization and the use of cryoprotectants are significative in the formulation process. The use of cryoprotectants, even in smaller mass ratios, help to maintain the size of nanoparticles after the lyophilization process. In summary, we conclude that uniform nanoparticles can be successfully prepared by adjusting the formulation parameters in both techniques. Moreover, physicochemical characteristics show to be suitable for therapeutic use, by obtaining uniform size, stable and reproducible nanoparticles. Also, the PNP preparation is sensitive to modifications in almost every step of the formulation, purification, and storage process. Therefore, by adjusting the parameters mentioned above, both techniques have the potential to be tuned to obtain any final nanoparticle desired characteristics, while maintaining reproducible results.

Conflicts of interest

There are no conflicts to declare.

Acknowledgements

Karol Yesenia Hernández-Giottonini, Rosalva Josefina Rodríguez-Córdova, and Omar Peñuñuri-Miranda thanks CONACYT for the graduate scholarships 302373, 281669, and 638788 respectively.

References

1 B. Kumar, K. Jalodia, P. Kumar and H. K. Gautam, *J. Drug Delivery Sci. Technol.*, 2017, **41**, 260–268.
2 S. Patel, D. Singh, S. Srivastava, M. Singh, K. Shah, D. Chauahn and N. Chauhan, *Adv. Pharmacol. Pharm.*, 2017, **5**, 31–43.
3 J. Ghitman, R. Stan and H. Iovu, *UPB Scientific Bulletin, Series B: Chemistry and Materials Science*, 2017, **79**, 101–112.
4 J. D. Robertson, L. Rizzello, M. Avila-Olias, J. Gaitzsch, C. Contini, M. S. Magón, S. A. Renshaw and G. Battaglia, *Sci. Rep.*, 2016, **6**, 1–9.
5 K. M. El-say and H. S. El-sawy, *Int. J. Pharm.*, 2017, **528**, 675–691.
6 D. Y. Chung, S. W. Jun, G. Yoon, H. Kim, J. M. Yoo, K. S. Lee, T. Kim, H. Shin, A. K. Sinha, S. G. Kwon, K. Kang, T. Hyeon and Y. E. Sung, *J. Am. Chem. Soc.*, 2017, **139**, 6669–6674.
7 P. L. Saldanha, V. Lesnyak and L. Manna, *Nano Today*, 2017, **12**, 46–63.
8 C. Gutiérrez-Valenzuela, P. Guerrero-Germán, A. Tejeda-Mansir, R. Esquivel, R. Guzmán-Z and A. Lucero-Acuña, *Appl. Sci.*, 2016, **6**, 1–15.
9 M.-Y. Hsu, C.-H. Feng, Y.-W. Liu and S.-J. Liu, *Appl. Sci.*, 2019, **9**, 1077.
10 B. Colzani, L. Pandolfi, A. Hoti, P. A. A. Iovene, A. Natalello, S. Avvakumova, M. Colombo and D. Prosperi, *Int. J. Nanomed.*, 2018, **13**, 957–973.
11 S. Rezvantalab, N. I. Drude, M. K. Moraveji, N. Güvener, E. K. Koons, Y. Shi, T. Lammers and F. Kiessling, *Front. Pharmacol.*, 2018, **9**, 1–19.
12 R. Goyal, L. K. Macri, H. M. Kaplan and J. Kohn, *J. Controlled Release*, 2016, **240**, 77–92.
13 X. Yang, Y. Chen, M. Wang, H. H. Zhang, X. Li and H. H. Zhang, *Adv. Funct. Mater.*, 2016, **26**, 8427–8434.
14 A. Lucero-Acuña, J. J. Jeffery, E. R. Abril, R. B. Nagle, R. Guzman, M. D. Pagel and E. J. Meuillet, *Int. J. Nanomed.*, 2014, **9**, 5653–5665.
15 S. Haque, B. J. Boyd, M. P. McIntosh, C. W. Pouton, L. M. Kaminskas and M. Whittaker, *Curr. Nanosci.*, 2018, **14**, 448–453.
16 A. Maaz, W. Abdelwahed, I. A. A. Tekko, S. Trefi, A. Maaz, W. Abdelwahed, I. A. Tekko and S. Tref, *International Journal of Academic Scientific Research*, 2015, **3**, 1–12.
17 S. Mallakpour and V. Behranvand, *eXPRESS Polym. Lett.*, 2016, **10**, 895–913.
18 F. Masood, *Mater. Sci. Eng., C*, 2016, **60**, 569–578.
19 J. Yang, S. Han, H. Zheng, H. Dong and J. Liu, *Carbohydr. Polym.*, 2015, **123**, 53–66.
20 H. A. Almoustafa, M. A. Alshawsh and Z. Chik, *Int. J. Pharm.*, 2017, **533**, 275–284.
21 S. Betala, M. M. Varma and K. Abbulu, *J. Drug Delivery Ther.*, 2018, **8**, 187–191.
22 W. Badri, K. Miladi, Q. A. Nazari, H. Fessi and A. Elaissari, *Colloids Surf., A*, 2017, **516**, 238–244.
23 H. Fessi, F. Puisieux, J. P. Devissaguet, N. Ammoury and S. Benita, *Int. J. Pharm.*, 1989, **55**, 1–4.
24 V. J. Pansare, D. Tien, P. Thoniyot and R. K. Prud'homme, *J. Membr. Sci.*, 2017, **538**, 41–49.
25 K. Nair, S. Vidyanand, J. James and G. S. Kumar, *J. Appl. Polym. Sci.*, 2012, **124**, 2030–2036.
26 C. Bouaoud, S. Xu, E. Mendes, J. G. J. L. Lebouille, H. E. A. De Braal and G. M. H. Meesters, *J. Appl. Polym. Sci.*, 2016, **133**, 1–11.
27 H. Mahdavi, H. Mirzadeh, H. Hamishehkar, A. Jamshidi, A. Fakhari, J. Emami, A. R. Najafabadi, K. Gilani, M. Minaiyan, M. Najafi, M. Tajarod and A. Nokhodchi, *J. Appl. Polym. Sci.*, 2010, **116**, 528–534.
28 S. A. Fahmy and W. Mamdouh, *J. Appl. Polym. Sci.*, 2018, **46133**, 1–9.
29 J. Tang, J.-Y. Chen, J. Liu, M. Luo, Y.-J. Wang, X. Wei, X. Gao, B. Wang, Y.-B. Liu, T. Yi, A.-P. Tong, X.-R. Song, Y.-M. Xie, Y. Zhao, M. Xiang, Y. Huang and Y. Zheng, *Int. J. Pharm.*, 2012, **431**, 210–221.
30 C. G. Keum, Y. W. Noh, J. S. Baek, J. H. Lim, C. J. Hwang, Y. G. Na, S. C. Shin and C. W. Cho, *Int. J. Nanomed.*, 2011, **6**, 2225–2234.
31 S. A. Joshi, S. S. Chavhan and K. K. Sawant, *Eur. J. Pharm. Biopharm.*, 2010, **76**, 189–199.
32 B. Sahana, K. Santra, S. Basu and B. Mukherjee, *Int. J. Nanomed.*, 2010, **5**, 621–630.

33 S. Jahan and A. Haddadi, *Int. J. Nanomed.*, 2015, **10**, 7371–7384.
34 J. Vandervoort and A. Ludwig, *Int. J. Pharm.*, 2002, **238**, 77–92.
35 T. Adebileje, A. Valizadeh and A. Amani, *J. Contemp. Med. Sci.*, 2017, **3**, 306–312.
36 M. Halayqa, U. Doma and U. Domańska, *Int. J. Mol. Sci.*, 2014, **15**, 23909–23923.
37 C. Fonseca, S. Simões and R. Gaspar, *J. Controlled Release*, 2002, **83**, 273–286.
38 S. Derman, *J. Nanomater.*, 2015, **2015**, 341848.
39 X. Song, Y. Zhao, S. Hou, F. Xu, R. Zhao, J. He, Z. Cai, Y. Li and Q. Chen, *Eur. J. Pharm. Biopharm.*, 2008, **69**, 445–453.
40 K. Dillen, J. Vandervoort, G. Van Den Mooter, L. Verheyden and A. Ludwig, *Int. J. Pharm.*, 2004, **275**, 171–187.
41 R. P. Darade, F. J. Sayyad and A. Patil, *Indo Am. J. Pharm. Res.*, 2014, **4**, 5111–5120.
42 M. S. Muthu, M. K. Rawat, A. Mishra and S. Singh, *Nanomedicine*, 2009, **5**, 323–333.
43 T. Govender, S. Stolnik, M. C. Garnett, L. Illum and S. S. Davis, *J. Controlled Release*, 1999, **57**, 171–185.
44 F. Madani, S. S. Esnaashari, B. Mujokoro, F. Dorkoosh, M. Khosravani and M. Adabi, *Adv. Pharm. Bull.*, 2018, **8**, 77–84.
45 S. A. Galindo-Rodríguez, F. Puel, S. Briançon, E. Allémann, E. Doelker and H. Fessi, *Eur. J. Pharm. Sci.*, 2005, **25**, 357–367.
46 Z. He, H. Huang, J. L. Santos, Y. Chen, K. W. Leong, Y. Hu, L. Liu, H.-Q. Mao and H. Tian, *Biomaterials*, 2017, **130**, 28–41.
47 S. Pieper and K. Langer, *Mater. Today: Proc.*, 2017, **4**, S188–S192.
48 E. Sah and H. Sah, *J. Nanomater.*, 2015, **2015**, 1–22.
49 C. E. Mora-huertas, O. Garrigues, H. Fessi and A. Elaissari, *Eur. J. Pharm. Biopharm.*, 2012, **80**, 235–239.
50 R. Paliwal, R. J. Babu and S. Palakurthi, *AAPS PharmSciTech*, 2014, **15**, 1527–1534.
51 A. Lucero-Acuña and R. Guzmán, *Int. J. Pharm.*, 2015, **494**, 249–257.
52 S. Xie, S. Wang, B. Zhao, C. Han, M. Wang and W. Zhou, *Colloids Surf., B*, 2008, **67**, 199–204.
53 C. E. Astete and C. M. Sabliov, *J. Biomater. Sci., Polym. Ed.*, 2006, **17**, 247–289.
54 H. Y. Kwon, J. Y. Lee, S. W. Choi, Y. Jang and J. H. Kim, *Colloids Surf., A*, 2001, **182**, 123–130.
55 R. M. Mainardes and R. C. Evangelista, *Int. J. Pharm.*, 2005, **290**, 137–144.
56 M. C. Operti, D. Fecher, E. A. W. van Dinther, S. Grimm, R. Jaber, C. G. Figdor and O. Tagit, *Int. J. Pharm.*, 2018, **550**, 140–148.
57 C. Rodrigues de Azevedo, M. von Stosch, M. S. Costa, A. M. Ramos, M. M. Cardoso, F. Danhier, V. Préat and R. Oliveira, *Int. J. Pharm.*, 2017, **532**, 229–240.
58 A. Frank, S. K. Rath and S. S. Venkatraman, *J. Controlled Release*, 2005, **102**, 333–344.
59 J. Herrmann and R. Bodmeier, *J. Controlled Release*, 1995, **36**, 63–71.
60 R. P. Félix Lanao, A. M. Jonker, J. G. C. Wolke, J. A. Jansen, S. C. G. Van Hest and J. C. M. Leeuwenburgh, *Tissue Eng., Part B*, 2013, **19**, 380–390.
61 R. H. Ansary, M. B. Awang and M. M. Rahman, *Trop. J. Pharm. Res.*, 2014, **13**, 1179–1190.
62 J. Panyam, D. Williams, A. Dash, D. Leslie-Pelecky and V. Labhasetwar, *J. Pharm. Sci.*, 2004, **93**, 1804–1814.
63 F. Lince, D. L. Marchisio and A. A. Barresi, *J. Colloid Interface Sci.*, 2008, **322**, 505–515.
64 X. Wu, Y. Chang, Y. Fu, L. Ren, J. Tong and J. Zhou, *Starch/Staerke*, 2016, **68**, 258–263.
65 H. Rachmawati, Y. L. Yanda, A. Rahma and N. Mase, *Sci. Pharm.*, 2016, **84**, 191–202.
66 J. Vysloužil, P. Doležel, M. Kejdušová, E. Mašková, J. Mašek, R. Lukáč, V. Košťál, D. Vetchý and K. Dvořáčková, *Acta Pharm.*, 2014, **64**, 403–417.
67 K. Miladi, S. Sfar, H. Fessi and A. Elaissari, *Ind. Crops Prod.*, 2015, **72**, 24–33.
68 A. Lamprecht, N. Ubrich, M. H. Perez, C.-M. Lehr, M. Hoffman and P. Maincent, *Int. J. Pharm.*, 2000, **196**, 177–182.
69 S. K. K. Sahoo, J. Panyam, S. Prabha and V. Labhasetwar, *J. Controlled Release*, 2002, **82**, 105–114.
70 E. Chiesa, R. Dorati, T. Modena, B. Conti and I. Genta, *Int. J. Pharm.*, 2018, **536**, 165–177.
71 H. Murakami, M. Kobayashi, H. Takeuchi and Y. Kawashima, *Int. J. Pharm.*, 1999, **187**, 143–152.
72 A. Maaz, W. Abdelwahed, I. A. Tekko and S. Trefi, *International Journal of Academic Scientific Research*, 2015, **3**, 1–12.
73 S. M. Habib, A. S. Amr and I. M. Hamadneh, *J. Am. Oil Chem. Soc.*, 2012, 695–703.
74 H. Wang, Y. Jia, W. Hu, H. Jiang, J. Zhang and L. Zhang, *Pharmaceut. Dev. Technol.*, 2013, **18**, 694–700.
75 S. A. Guhagarkar, V. C. Malshe and P. V Devarajan, *AAPS PharmSciTech*, 2009, **10**, 695–703.
76 S. Das, P. K. Suresh and R. Desmukh, *Nanomedicine*, 2010, **6**, 318–323.
77 Sonam, H. Chaudhary and V. Kumar, *Int. J. Biol. Macromol.*, 2014, **64**, 99–105.
78 A. M. De Oliveira, E. Jäger, A. Jäger, P. Stepánek and F. C. Giacomelli, *Colloids Surf., A*, 2013, **436**, 1092–1102.
79 T. Kantaria, T. Kantaria, S. Kobauri, M. Ksovreli, T. Kachlishvili, N. Kulikova, D. Tugushi and R. Katsarava, *Appl. Sci.*, 2016, **6**, 444.
80 J. Cheng, B. A. Teply, I. Sherifi, J. Sung, G. Luther, F. X. Gu, E. Levy-Nissenbaum, A. F. Radovic-Moreno, R. Langer and O. C. Farokhzad, *Biomaterials*, 2007, **28**, 869–876.
81 W. Huang and C. Zhang, *Biotechnol. J.*, 2018, **13**, 1–19.
82 N. Morsi, D. Ghorab, H. Refai and H. Teba, *Int. J. Pharm.*, 2016, **506**, 57–67.
83 A. Malkani, A. A. Date and D. Hegde, *Drug Delivery Transl. Res.*, 2014, 365–376.
84 P. Hassanzadeh, I. Fullwood, S. Sothi and D. Aldulaimi, in *Gastroenterology and Hepatology from Bed to Bench*, 2011, vol. 4, pp. 63–69.

85 R. S. Dangi and S. Shakya, *Int. J. Pharm. Life Sci.*, 2013, **4**, 2810–2818.
86 V. G. Kadajji and G. V. Betageri, *Polymers*, 2011, **3**, 1972–2009.
87 H. Katas, E. Cevher and H. O. Alpar, *Int. J. Pharm.*, 2009, **369**, 144–154.
88 J. P. Rao and K. E. Geckeler, *Prog. Polym. Sci.*, 2011, **36**, 887–913.
89 M. Azizi, F. Farahmandghavi, M. Joghataei, M. Zandi, M. Imani, M. Bakhtiary, F. A. Dorkoosh and F. Ghazizadeh, *J. Polym. Res.*, 2013, **20**, 1–14.
90 D. Moinard-Chécot, Y. Chevalier, S. Briançon, L. Beney and H. Fessi, *J. Colloid Interface Sci.*, 2008, **317**, 458–468.
91 K. Narayanan, V. M. Subrahmanyam and J. V. Rao, *Enzyme Res.*, 2014, **2014**, 162962.
92 M. Nahar and N. K. Jain, *Pharm. Res.*, 2009, **26**, 2588–2598.
93 S. Dyawanapelly, U. Koli, V. Dharamdasani, R. Jain and P. Dandekar, *Drug Delivery Transl. Res.*, 2016, **6**, 365–379.
94 R. Donno, A. Gennari, E. Lallana, J. M. Rios De La Rosa, R. D'Arcy, K. Treacher, K. Hill, M. Ashford and N. Tirelli, *Int. J. Pharm.*, 2017, **534**, 97–107.
95 D. H. Abdelkader, S. A. El-Gizawy, A. M. Faheem, P. A. McCarron and M. A. Osman, *J. Drug Delivery Sci. Technol.*, 2018, **43**, 160–171.
96 S. Prabha and V. Labhasetwar, *Pharm. Res.*, 2004, **21**, 354–364.
97 A. Budhian, S. J. Siegel and K. I. Winey, *Int. J. Pharm.*, 2007, **336**, 367–375.
98 N. Sharma, P. Madan and S. Lin, *Asian J. Pharm. Sci.*, 2016, **11**, 404–416.
99 A. Tripathi, R. Gupta and S. A. Saraf, *Int. J. PharmTech Res.*, 2010, **2**, 2116–2123.
100 C. Fornaguera and C. Solans, *Int. J. Polym. Sci.*, 2018, **2018**, 1–10.
101 C. Vauthier and K. Bouchemal, *Pharm. Res.*, 2009, **26**, 1025–1058.
102 H. Katas, S. H. U. Chen, A. A. Osamuyimen, E. Cevher and H. O. Y. A. Alpar, *J. Microencapsulation*, 2008, **25**, 541–548.
103 I. Takeuchi, S. Kobayashi, Y. Hida and K. Makino, *Colloids Surf., B*, 2017, **155**, 35–40.
104 H. Murakami, Y. Kawashima, T. Niwa, T. Hino, H. Takeuchi and M. Kobayashi, *Int. J. Pharm.*, 1997, **149**, 43–49.
105 C. Pinto Reis, R. J. Neufeld, A. J. Ribeiro and F. Veiga, *Nanomedicine*, 2006, **2**, 8–21.
106 W. Abdelwahed, G. Degobert and H. Fessi, *Int. J. Pharm.*, 2006, **324**, 74–82.
107 P. Fonte, S. Soares, A. Costa, J. C. Andrade, V. Seabra, S. Reis and B. Sarmento, *Biomatter*, 2012, **2**, 329–339.
108 M. Holzer, V. Vogel, W. Mäntele, D. Schwartz, W. Haase and K. Langer, *Eur. J. Pharm. Biopharm.*, 2009, **72**, 428–437.
109 A. Rampino, M. Borgogna, P. Blasi, B. Bellich and A. Cesàro, *Int. J. Pharm.*, 2013, **455**, 219–228.
110 K. S. Tang, S. M. Hashmi and E. M. Shapiro, *Nanotechnology*, 2013, **24**, 1–19.
111 A. Saez, M. Guzmán, J. Molpeceres and M. R. Aberturas, *Eur. J. Pharm. Biopharm.*, 2000, **50**, 379–387.